

We are IntechOpen, the world's leading publisher of Open Access books Built by scientists, for scientists

6,900

Open access books available

186,000

International authors and editors

200M

Downloads

Our authors are among the

154

Countries delivered to

TOP 1%

most cited scientists

12.2%

Contributors from top 500 universities



WEB OF SCIENCE™

Selection of our books indexed in the Book Citation Index
in Web of Science™ Core Collection (BKCI)

Interested in publishing with us?
Contact book.department@intechopen.com

Numbers displayed above are based on latest data collected.
For more information visit www.intechopen.com



Electrodeposition of Thin Films for Low-cost Solar Cells

Abhijit Ray

Additional information is available at the end of the chapter

<http://dx.doi.org/10.5772/61456>

Abstract

This chapter endeavors to bring to the reader the potential of electrochemical deposition processes to develop low cost solar cells. The targeted photovoltaic absorbers are largely inorganic compound semiconductors containing earth abundant elements and satisfying the physical criteria of band gap and dopability. Electrodeposition, being an well established chemical process having its inherent capability for a large productions, should also be applied to develop various low cost solar cells, such as $\text{Cu}_2\text{ZnSnS}_4$, Cu_2S , FeS_2 , Zn_3P_2 , few/mono-layer MoS_2 and WS_2 etc having direct band gaps and ability to engineer their band gap through in-situ doping for creating various possible hereojunctions. The author believes that the combined effort of electrochemistry, physics and chemical engineering can push this simple and ultra-low cost technique of electrodeposition along with other supporting solution based techniques to produce PV energy at most affordable price in coming days.

Keywords: Solar cells, Electrodeposition, Thin films

1. Introduction

Despite the fact that, solar photovoltaic (PV) devices and modules made from crystalline (poly/mono) Silicon dominate the market at present, a significant efforts are underway in developing alternative materials to reduce dependence on Silicon [1,2] and bring them in the form of thin films to reduce the module cost [3,4]. Such non-silicon materials satisfying the prime requirement of right optical band gap (between 1-1.6eV) and high absorption coefficients (in the case of direct band gap semiconductors) [5] in the visible solar spectrum are usually binary or multinary alloys or compounds [6]. In most of the cases, their heterojunctions with a wide band gap emitter layer are exploited in the solar cells as their band gap can be tuned to a desired level by varying the compositions [7-9]. Because of the stoichiometry and stability of these materials are a primary concern to fabricate a successful junction [10,11], they are usually

grown by highly controlled vacuum environments, such as the vacuum evaporation [12,13], chemical vapor deposition (CVD) [14-17], molecular beam epitaxy (MBE) [18], or sputtering [19-21] techniques. Besides the high energy requirement for the above film processing, emission of gaseous waste materials is another serious issue with these techniques [22,23]. These materials can also be deposited in thin films from solution in so called 'wet process' having the advantage of 'low energy' and 'low waste', provided the chemical environment allows a controlled ionization and subsequent reactions to form the compound film with required stoichiometry [24-26]. Among wet processes, spin coating [27], ink printing [28,29], chemical spray pyrolysis [30-32], successive ionic layer adsorption and reaction (SILAR) [33], chemical bath deposition (CBD) [34] and electrochemical deposition or electrodeposition (ED) [35,36]. In general, thin films deposited by ED method do not possess the high crystalline perfection as that made from CVD or MBEs. However, it has appeared as an attractive method owing to the involvement of cheap capital equipment [37-39], associated scalability [40,41], low waste of precursors and no usage of air or carrier gasses in most cases [36,42]. In addition, for application in PV cells, ED process allows one to easily alter both the optical properties (band gap), electronic properties (carrier concentration, conductivity and mobility) and structure (lattice constant) by the composition modulation through the control of bath parameters, such as applied potential (magnitude and type – dc or pulse), pH, and temperature of the bath, use of agitation (stirring) or excitation (such as by applying light). A number of largely cited ED processes for the synthesis of various low cost compound semiconductors for photovoltaic applications, their reported optical band gap and champion cell efficiencies are summarized in Table-1. Thus, the electrodeposition technique deserves its place for large scale commercialization of various new PV devices and modules of lower cost than Silicon counterpart in future. The present chapter brings to the reader's attention, the common aspects of electrodeposition technique and its application in some specific PV absorber materials.

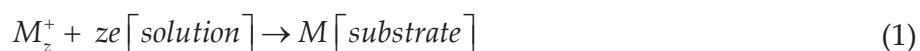
System	Research group	Year	Method of electrodeposition	Obtained band gap (eV)	Best cell efficiency reported (%)	Reference
Cu ₂ S	Anwar <i>et al.</i>	2002	Cathodic	-	-	[155]
Cu ₂ SnS ₃	Koike <i>et al.</i>	2012	Potentiostatic, single step	-	2.84	[156]
	Mathews <i>et al.</i>	2013	Potentiostatic, stacking metallic layers	1	-	[157]
Cu ₂ ZnSnS ₄	Mkawi <i>et al.</i>	2014	Pulsed electrodeposition	1.36-1.47	1.66	[172]
	Araki <i>et al.</i>	2009	Potentiostatic, single step	-	0.98	[92]
	Ennaoui <i>et al.</i>	2009	Potentiostatic, single step	1.54	3.4	[36]
	Sheng <i>et al.</i>	2012	Potentiostatic, single step using ionic liquid	1.51	-	[158]
	Ahmed <i>et al.</i>	2012	Potentiostatic, stacking mettalic layers	1.48-1.6	7.3	[130]

System	Research group	Year	Method of electrodeposition	Obtained band gap (eV)	Best cell efficiency reported (%)	Reference
	Cui <i>et al.</i>	2011	Potentiostatic, single step	1.5	-	[159]
	Pawar <i>et al.</i>	2011	Potentiostatic, single step	1.48-1.76	-	[160]
	Chan <i>et al.</i>	2010	Potentiostatic, single step using ionic liquid	1.49-1.5	-	[154]
Cu ₂ ZnSnSe ₂	Jeon <i>et al.</i>	2014	Potentiostatic, single step	1.04	8	[161]
	Zhang <i>et al.</i>	2013	Potentiostatic, single step	0.98	4.5	[129]
	Guo <i>et al.</i>	2012	Potentiostatic, stacking mettalic layers	1.29	7	[162]
	Septina <i>et al.</i>	2013	Potentiostatic, single step	1.41-1.48	-	[163]
	Li <i>et al.</i>	2012	Potentiostatic, single step	1	1.7	[164]
SnS	Seichen <i>et al.</i>	2013	Cathodic	-	-	[165]
	Ghazali <i>et al.</i>	1998	Cathodic	1.1	-	[166]
	Subramanian <i>et al.</i>	2001	Cathodic	1.15	-	[167]
	Zainal <i>et al.</i>	1996	Cathodic	-	-	[168]
	Cheng <i>et al.</i>	2006	Galvanostatic (constant current)	1.21-1.42	-	[169]
	Cheng <i>et al.</i>	2007	Pulsed electrodeposition	1.23-1.33	-	[170]
	Cheng <i>et al.</i>	2006	Cathodic	1.48-1.24	-	[171]

Table 1. Various reported electrodeposition (ED) routes for fabrication of some low cost photovoltaic grade thin films and their associated properties. Although several other systems including CuIn(S/Se)₂, Cu(In,Ga)(S/Se)₂, GaAs etc have been attempted via electrodeposition, they are not listed below as they either involve expensive precursors or post treatment.

2. Electrodeposition

Electrodeposition of metals and alloys on a conducting substrate involves the reduction of metal ions from various possible electrolytes, such as aqueous, non-aqueous, organic, ionic liquids and molten salts. In general the reduction of a cation species present in the aqueous solution with z positive charge, M_z^+ to produce a neutral metal atom M on the cathode as substrate is represented by,



In above reaction, the charges are provided by an external current source and a layer of M atoms are deposited in an allowed time. More is the concentration of M_z^+ , larger will be the number of M atoms deposited onto the substrate to form a lattice eventually.

2.1. Common aspects

In the reaction given by Eq. 1, the process involves charged species at the interface between a solid conducting electrode and a liquid solution. These charged species are obviously the cations and electrons, which cross the interface. There are usually four types of primary characteristics associated to Eq. 1 which are commonly dealt in the case of electrodeposition [43]: 1. *Interface between metal and solution*. Here crystal structure and electronic properties of the metal, molecular structure of the polar solvent (in case of aqueous medium), and the structure and properties of the electrolyte used are the governing factors. 2. *Rate of the deposition process*. This is proportional to the concentration of the active cations in the solution available for reduction by the electrons supplied by the cathode. A proportionality constant can be referred to as 'rate constant', k that is defined in terms of an electrochemical activation energy, ΔG_e which in turn is determined as a function of the electrode potential, E through following set of equations:

$$k = \frac{k_B T}{h} \ln \left(-\frac{\Delta G_e}{RT} \right) \quad (2)$$

$$\Delta G_e = f(E) \quad (3)$$

3. *Nucleation and growth mechanism*. As the ions reach the electrode surface for reduction the surface nuclei can grow in one, two or three dimension as determined by the parameters of the electrodeposition and nature of the solution. This may lead to the formation of monolayer, few layers, multilayers or three dimensional growths depending on the mode of nucleation. 4. *Structure and physico-chemical properties of the deposit*. Crystal structure, microstructure and elementary composition of the deposit under a certain growth condition will determine the physical (such as, electrical, mechanical, optical etc.) as well as chemical (such as, reactivity to its ambient, stability etc.) properties of the film which is desired for an application or required to be looked at to prevent certain unwanted effect during an application. A more detail of nucleation and growth mechanism is given in reference [43] and in the subsequent section in brief.

2.2. Nucleation and growth mechanisms

The electrodeposition process attains a dynamic equilibrium among the metal cations, electrons participating in the reduction process and the metal atoms to be deposited on the cathode surface. With the establishment of this dynamic equilibrium, fully solvated (water molecules attached to it in case of an aqueous electrolyte or ligands in the case of use of complexing agents) ions get attracted towards the oppositely charged electrode surface by coulombic forces as shown in Fig. 1 in the case of cations, for example. Eventually an electrical double layer is formed, where the inner layer is largely composed of oriented water dipoles interposed by some preferentially adsorbed ions and the outer layer is a jacket of ions having

charge opposite to that of the electrode. These cations are adsorbed onto the cathode surface by displacing the attached water molecules or ligands. Upon a continuous depletion of the depositing ions from the double layer region, fresh ions are supplied from the bulk of electrolyte by either or mix of three important processes: (i) diffusion due to concentration gradient, (ii) electric field assisted migration and (iii) convection current in the electrolyte due to temperature or agitations.

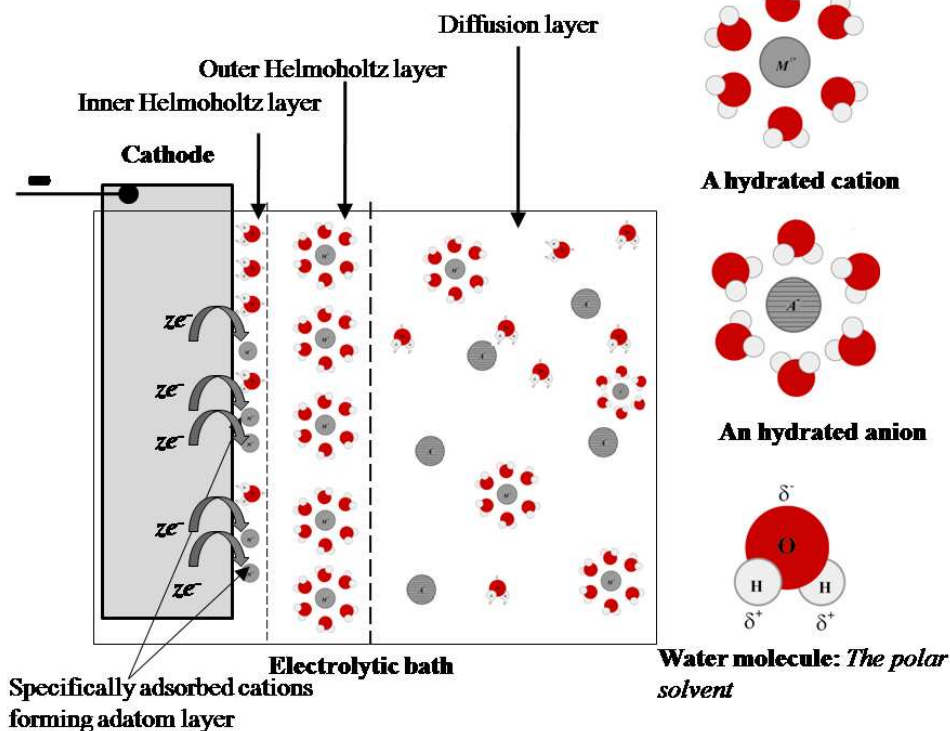


Figure 1. Illustration of a fundamental cathodic electrodeposition process at for a single constituent metal salt dissolved in an aqueous electrolyte

Some of the process parameters critically determine the growth of the deposits, such as current density through the electrode, electrolytic bath condition, shape of the active electrode and type and shape of the counter electrode. The current density determines in particular, the rate of deposition and hence microstructure the deposited film. An optimum range of current density is determined experimentally for each of the depositing ion species by electrochemical characterizations technique. Bath parameters, such as the concentration of individual ion species, use of complexing agents and their concentration, temperature, illumination or irradiation influences the nucleation process as these parameters can directly influence the inner row (Stern layer) of the Helmholtz double layer. Bath temperature controls the rate of diffusion of the ions from the diffusion to Helmholtz layer, the convection current, stability of any complex and decomposition of any additive used. The shape of the active electrode sometimes determines the thickness uniformity of the deposits. Higher current density at the edges or projections as compared to the crevices and hollow spaces leads to the formation of

thicker growth at the edges. The counter electrode is used to complete the circuit and balance the charge in dynamic process during electrodeposition. As the number of anions and OH⁻ remains very high as compared to the positive ions and protons as in the case of cathodic deposition, the counter electrode area becomes an important factor. Usually, a counter electrode area should be as large as four times the geometric surface area of the active electrode.

2.3. Cathodic electrodeposition

Cathodic electrodeposition, that means the deposition of thin film on the cathode surface is especially important for the single as well as multilayered metals or alloys deposition for compound semiconductor thin films for solar cells, photoelectrochemical (PEC) cells and photocatalytic action in Hydrogen Evolution Reaction (HER) in the case of PEC water splitting. The electrodeposition of an alloy requires their ions must be present in an electrolyte where the individual deposition potentials can be made to be close or even the same at the best.

There are three main steps must be followed in a cathodic electrodeposition process:

1. *Ionic migration:* The hydrated ion(s) in the electrolyte migrate(s) toward the cathode under the influence of an applied potential as well as through diffusion and/or convection.
2. *Electron transfer:* At the cathode surface the hydrated metal ion(s) enter(s) the diffusion (double) layer where the water molecules of the hydrated ion are aligned by the weak field present in this layer. Eventually, the metal ion(s) enter(s) the fixed Helmholtz layer, where, due to the higher field present, the hydrated shell is lost. Subsequently, the individual ion is neutralized by electron transfer from cathode and is adsorbed at the cathode surface.
3. *Incorporation:* In this last step the adsorbed atom is drifted to a growth point on the cathode and is incorporated in the growing lattice. The process continues, largely, as long as the applied potential is near to the reduction potential(s) of the ion(s).

The replenishment of the metal ions M_z^+ can be possible in two ways: 1. M_z^+ from an anode of M : the metal to be deposited is used as anode, when a metal ion is produced from some surface atoms in the metal lattice leaving back the electron(s) to anode. 2. M_z^+ from a salt of M : the anode can be made of a metal or conducting electrode other than M , a Pt electrode in most of the cases.

At the same time, ions from the solution are deposited on the electrode, according to step 2 above. The specific potentials at which these two reaction rates are equal, called *standard potentials*, which are defined for solutions maintained at 25°C and at an activity value of unity. Again, as the above two processes (oxidation-reduction) are reversible, the equilibrium potential at the metal electrode is given by the well known *Nernst expression*:

$$E = E^0 + \frac{RT}{zF} \ln Q \quad (4)$$

Here, E^0 is the *standard oxidation/reduction potential* for the electrode immersed in a solution of ions having unit activity, R is the gas constant, T is the temperature, z represents the number of valence electrons participating in the redox process, F is the Faraday constant ($F = 9.648\,533\,99(24) \times 10^4 \text{ C mol}^{-1}$) and Q is the reaction quotient that may be defined as the ratio of concentration of oxidized to that of the reduced ion species, that is usually taken as the activity of the reactant ions (a). However, the deposition, as a rule is an irreversible process that has to occur at some extra potential, E_{over} (overpotential) required for maintaining the reduction reaction and therefore, Eq. (4) should be written as,

$$E_{dep} = E^0 + \frac{RT}{zF} \ln a^{z+} + E_{over} \quad (5)$$

In practice, the metal deposition potential, E_{dep} can be estimated easily by cyclic voltammetry technique by knowing the values of a^{z+} and E_{over} for a fixed plating condition, including bath parameters, such as the current density and temperature, as well as the ionic parameters, such as solution pH , concentration, valence, and mobility.

In some cases of alloy deposition, when the standard electrode potential of more than one types of ions are widely different, such as in the case of $Zn^{2+} \rightarrow Zn$ and $Cu^{2+} \rightarrow Cu$, $E_0^{Zn^{2+};Zn} = -0.762V$ and $E_0^{Cu^{2+};Cu} = -0.345V$, respectively, their co-electrodeposition is apparently impossible. However, the difference can be eliminated (or reduced) by changing the values of the activities. This can be achieved by introducing a considerable change in ionic concentrations via complex ion formation.

2.3.1. Factors affecting the cathodic electrodeposition

In the case of aqueous electrolytes used in the electrodeposition, hydrogen evolution at the cathode is a common problem as the hydrogen evolution reaction (reduction of a proton released from water molecule by an electron) is pH dependent and it can occur simultaneously with the adsorption of cations and their reduction by electrons. This may cause pitting of the deposited thin film and worsening of its morphology. In order to prevent this hydrogen accumulation, a suitable wetting agent may be used to promote detachment of the H_2 evolved at the cathode. Sometimes by the use of ionic liquid or non-aqueous electrolyte, the H_2 evolution can be prevented. The control of pH in electrodeposition is important. The pH controls the overall conductivity of the electrolyte. If the electrolyte by itself is not very conductive, a suitable acid or alkali or salt may be used to achieve required conductivity. However, the pH is required to be optimized for an electrodeposition, because a low pH of solution may result only H_2 evolution, whereas a high pH may cause the inclusion of $-OH$ group in the deposits.

Current density plays an important role on the deposits. Use of low current densities, in general, result in higher impurities in the deposit, which in turn affects residual stress and other properties of the deposit. The flatness of the cathode surface (substrate used) also plays

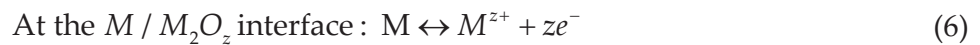
an important role in the case of alloy deposition, in general. An uneven surface leads to the variation of current densities and hence, the throwing power. In the case of inferior throwing power, the result may be uneven alloy composition on the cathode.

2.4. Anodization

The anodization is an important age-old electrochemical technique that has long been used for increasing the corrosion and wear resistance of various metal surfaces. It is an electrolytic surface passivation technique used to increase the thickness of native oxide layer on the surface of metal under the application of a large bias. Usually few tens of volts are required to maintain the oxidation reaction on the surface of anode. Eventually thickness of the oxide layer increases. Anodization changes the preferential crystal orientation (microscopic texture) of the surface and sometimes changes the crystal structure of the metal near the surface. The anodized surface retains its mechanical strengths and it can sustain mechanical deformation easily. Depending on the applied potential and anodization time, it may be referred to as 'soft' or 'hard' anodization. In the case of soft anodization, the formed layers are thin and usually compact, whereas in the case of hard anodization, they are thicker and many a times porous or template structure. While the former has certain importance in hardening the metal surface, the latter is useful in producing nano-structure templates in the case of many functional thin films including the thin film nanostructured solar cells.

2.4.1. Basics of anodization processes

A standard anodization procedure includes three important steps: 1. alkaline cleaning, 2. acid activation, and 3. biasing and reaction. After cleaning the anode surface (where film is required), acid treatment is given to the surface in a mixture of nitric acid (HNO_3) and hydrofluoric acid (HF) to remove the native metal oxide layer and surface contaminants. The biasing and anode reaction are carried out in an electrochemical bath, which usually has a three-electrode configuration (metal anode, platinum cathode and Ag/AgCl reference electrode). When a constant voltage (potentiaostatic condition) or current (galvanostatic condition) is applied between the anode and cathode, electrode redox reactions along with the field-driven ion diffusion lead to the formation of an oxide layer on the anode surface. The redox reactions for anodizing of a metal M with z nos of valence electrons therefore can be expressed as,



At the Ti oxide/electrolyte interface:



At both interfaces:



Some time due to the higher resistivity of the metal oxide film than the electrolyte and the metallic substrate, the deposition current density drops over time as the oxide film grows on the anode. As long as the electrical field is strong enough to drive the ion conduction through the oxide, the film keeps growing. For this reason, a large bias (even larger than the water splitting potential) is maintained. Obviously, the final oxide thickness, d is almost linearly dependent on the applied voltage, V_{app} according to:

$$D \sim aV_{app} \quad (10)$$

Where a is usually a constant lying the range 1.5-3 nm/V.

The physical and chemical properties (such as degree of nanometer roughness, morphology, stoichiometry, etc.) of the anodized film varies over a wide range according to different process parameters, such as applied potential (voltage), current density, electrolyte composition, pH, and temperature. If the applied voltage exceeds the dielectric breakdown limit (DBL) of the oxide, it will no longer be resistive to prevent further current flow. Eventually, it leads to more gas revolution and sparking, resulting degradation of film quality. However, the DBL varies in various electrolytes [44]. In their study, it was shown that, below the DBL, the anodic oxide film is thin and usually non-porous using non-fluorine electrolytes. A constant temperature during the anodization process is usually preferred to maintain a homogeneous field-enhanced dissolution over the entire area of anode. Since increased temperature accelerates the chemical dissolution rate, the working temperature is often kept relatively low to prevent the oxide from totally dissolving. Nature of the electrolyte has been found to have great effect as well. Sul *et al.* [45] have shown highest thickness of anodized TiO₂ film is obtained when H₂SO₄ is used.

2.4.2. Anodization used for solar cell fabrication

Anodization has reportedly been applied in various aspects of surface nano-engineering in solar cells and PEC cells through anodized TiO₂ nanostructure, anodic alumina (AAO) template etc. TiO₂ is a very suitable oxide material for dye-sensitized solar cells (DSSC), because of its extraordinary oxidizing ability of photogenerated holes. TiO₂ thin films are prepared by various preparation methods, but the efficiency of the DSSC is strongly enhanced by the increased dye absorption capacity of the photoelectrode and its nanostructure has been found to play a beneficial role [46,47]. Researchers have successfully adopted the anodization technique to grow the nanotube arrays from thin Ti films as well using anodization on a variety of substrates, such as glasses [58-60], conducting glass (FTO) [51-53], and silicon [54-56]. Another application of anodization is the removal through dissolution to produce rough

surfaces, which are sometime very useful in creating anti-reflection coating as well as nano-structure to enhance optical path through scattering for solar cells. In this direction, a significant improvement of light management for a:Si solar cell was reported by Huang *et al.* [57] where they reported the use of AAO template to deposit Ag nano-back reflector to improve optical path in the system. It was reported to improve the photo conversion efficiency from 6.64% to 7.11% in a:Si solar cells. Wang *et al.* [58] used AAO template to produce nano-wire of $\text{Cu}_2\text{ZnSnS}_4$ which is a direct band gap photovoltaic absorber. Anodized ZnO post doped with Al has proved to be an excellent textured transparent conducting oxide (TCO) layer for thin film silicon solar cells [59].

2.4.3. Anodic vs. Cathodic Electrodepositions of compound semiconductors for solar or PEC cells

In principle, both anodic and cathodic deposition may be used for the fabrication of compound semiconductor for thin film solar cells. However, there are two issues with anodic deposition. Firstly the stoichiometry of the compound may change over time of deposition, as the anions available from the solution are only available to participate in the redox reaction at the metal anode, such as in the case of CdS, CdTe, ZnTe etc. Secondly, if more than one metal components are required in the film, such as the ternary or quaternary compounds like CuIn(S/Se)_2 , $\text{Cu}_2\text{ZnSn(S/Se)}_2$ etc anodic deposition is not much suitable and cathodic deposition can handle all the cationic components in solution easily provided their reduction potential can be made close. It has been reported that CdS can be made by the anodic deposition of sulphur from a solution containing S^{2-} ions on a cadmium anode [60]. Similar anodic deposition has been attempted for CdTe films [61] as well, however, the stoichiometry of the deposit was not easy to regulate. However, if each element of a semiconducting material (e.g. Cd and Te for CdTe, or Cd and S for CdS) can be deposited cathodically, it may be possible to deposit them in good stoichiometry. Cathodic deposition can occur either by deposition of the individual cation and anion components in the required ratio in a multi-step process, or by co-deposition resulting from mass transfer and decomposition of a complex containing the cation and anion components.

2.5. Pourbaix diagram and its application in electrodeposition

Prior to conducting an electrodeposition, the analysis of thermodynamic data obeying chemical and electrochemical equilibrium is highly helpful in understanding the reactivity of a compound system to be used for deposition of a desired phase. *Pourbaix* (potential–pH) diagrams [62] offers an excellent guideline about the detailed picture of the electrochemical solution growth system in terms of the deposition variables and reaction possibilities under different conditions of pH, redox potential, and/or concentrations of dissolved and electroactive species.

Pourbaix diagrams for a number of solar energy materials (such as, that for the aqueous Cd–S, Cd–Te, Cd–Se, Cu–In–Se, and Sb–S systems) have been presented and discussed in detail by Savadogo [63]. Pourbaix diagram is even more helpful in case, the system is partially substituted for an element by same group element for the purpose of doping. Dremlyuzhenko *et al.* [64] analyzed theoretically the mechanisms of redox reactions in the $\text{Cd}_{1-x}\text{Mn}_x\text{Te}$ and

Cd_{1-x}Zn_xTe aqueous systems and demonstrated the variation of physicochemical properties of the semiconductor surfaces as a function of solution pH. Pourbaix diagrams regarding compound semiconductors can be found from various literatures in the field of geochemistry, mineral processing, surface treatment and corrosion sciences. A number of important diagrams related to solar energy materials are reproduced in the reviews by Savadogo [63] and the monograph by Bouroushian [65].

2.6. Electrochemical epitaxy

The ordered growth of a single crystalline material on the top of a crystalline substrate is known as epitaxy, one of the important processes in semiconductor technology wherever crystalline thin films are required. Some of the most common epitaxial techniques are molecular beam epitaxy (MBE) [66], metal organic vapor phase epitaxy (MOVPE) [67] and liquid phase epitaxy (LPE) [68]. Among these techniques, the electrochemical atomic layer epitaxy (ECALE) is an LPE technique having two specific advantages over vacuum based epitaxy techniques, such as MBE and MOVPEs: 1. reduced cost of materials usage and operation, 2. ECALE is performed at room temperature or under the boiling point of the solvent, which are treated as “low temperature” deposition. The ECALE method is based on the alternate underpotential deposition (UPD) of the elements on a single crystal conducting substrate in a cycle [69]. The UPD is a surface-limited phenomenon, enabling the deposit to grow in atomic layers. Simply, the UPD is the one condition of deposition where an atomic layer of a first element is deposited on a second, at a potential prior to that needed to deposit the first element on itself. Thus each deposition cycle forms a monolayer of the compound, and the thickness of the deposit can be controlled by the number of deposition cycles. UPD is a thermodynamic phenomenon, where the interaction energy between the two elements is larger than that of an element with itself. Due to its formation on a single crystal surface, the resulting thin film consists of surface compound or alloy having same crystalline nature as that of the substrate.

In illustrative ECALE technique for form epitaxial CdS on (111) oriented Ag substrate (A detail of experimental conditions are described in ref. Innocenti, M., et al. [70]) is shown in Fig 2. The cycle is composed of four steps: reductive UPD of cadmium from a Cd²⁺ ion solution, a blank rinse, oxidative UPD of sulfur from a S²⁻ ion solution, and a second blank rinse. Separate solutions are used for each reactant and different potentials for each cycle step. The use of separate solutions and potentials provides extensive control over deposit growth, composition, and morphology. An atomic layer of S is deposited on one of Cd, and one of Cd is deposited on one of S according to following reactions:



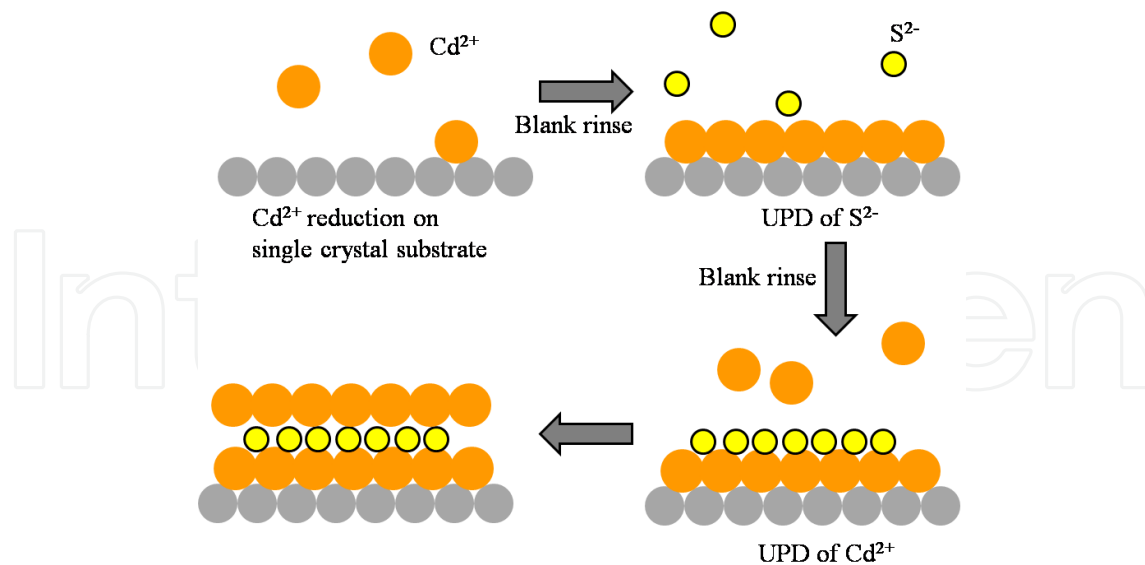


Figure 2. Illustration of an ECALE mechanism for deposition of CdTe thin film

A handful number of epi-films of compound semiconductors and solar energy materials have been attempted by various groups. Nanofilms of II-VI including ZnSe [71], CdTe [72,73], CdS [74-76], III-V compounds, such as InAs [77,78], and the photovoltaic absorber materials, such as CdTe [79], Ge, CIS, and CIGS.

3. Low cost thin film solar cells

Solar photovoltaics is projected to make a significant share of the world electricity production as the PV capacity is expected to grow up to 4.6TW worldwide by the year 2050 [80]. Inorganic thin-film semiconductor photovoltaic devices with a thickness of about 1 μm and efficiency of about 10% requires approximately, 10 g of active material per square meter, which corresponds to approximately 10 metric tons of the materials per GW production [6]. This estimate accounts to the requirement of an enormously large quantity of materials if a substantial share by thin films is to be considered, even though the material requirement is negligibly small as compared to bulk Silicon counterpart. Out of the presently commercially available thin-film materials, CdTe and $\text{Cu}(\text{In,Ga})(\text{Se,S})_2$ or CIGS, the elements Te, In, and Se are not abundant. Beside this, Indium used in Indium Tin Oxide (ITO) also has a large demand as the best performing transparent conducting electrode in many display devices. Therefore, a thin film photovoltaic technology beside their physical requirements (such as the optical band gap, absorption coefficient, intrinsic doping etc.) really demands its constituents to be abundant in earth crust (the relative abundance with respect to Silicon may be considered according to ref. [81]) as well as such elements have less superposition to other applications. By looking at the above aspects, a group of chalcogenides (CuS , Cu_2S , Cu_2SnS_3 , $\text{Cu}_2\text{ZnSnS}_4$, SnS , FeS_2 , MoS_2 and WS_2), oxides (CuO), silicides ($\beta\text{-FeSi}_2$, $\beta\text{-BaSi}_2$, Ca_2Si) and phosphides (CuP_2 , Zn_3P_2 , b-ZnP_2 , SiP) can be identified as potential thin film photovoltaic absorbers [82].

4. Electrodeposited thin film solar cells

The categories of semiconducting compounds listed in the previous section can be considered for thin film solar cells as most of them (such as, Cu_2SnS_3 , $\text{Cu}_2\text{ZnSnS}_4$, SnS , FeS_2 , Zn_3P_2 etc) have direct optical band gap and high absorption coefficients in the visible solar spectrum. However, for these compound semiconductors after synthesis to be useful as PV absorber, stringent requirements are to be met regarding structure, composition, and morphology. Although, simple by operation, it is a formidable challenge for any electrodeposition process to take care of all the above mentioned requirements simultaneously. In many cases, more than a single step deposition and/or additional post deposition treatments (surface treatment, annealing etc) are required before electrodeposited layers can be deployed in a solar cell. The post deposition annealing has a special role to improve both the crystallinity of the deposits and the optoelectronic properties of the layer. In order to electrodeposit a compound semiconductor thin film with *p*-type conductivity and grain size of approximately a micrometer directly, a number of criteria have to be fulfilled. The nucleation density should be low to moderate so that large grains can be grown uniformly, and any secondary nucleation should be avoided. At the same time, overlapping grains should not leave pinholes that lower the shunt resistance of the device, causing a very low short circuit current density of the final cell. The layer thickness should be uniform throughout the substrate to ensure low surface recombination losses, higher average generation of electron-hole pairs in order to produce higher open circuit voltage.

As mentioned above, the requirement for strict control of stoichiometry has three important trade-offs: **1.** Electrons need to be readily available for the reduction of precursor ionic species at cathode (in the case of cathodic deposition) Again, free holes produced from photo- or thermal-excitation at the *p*-type layer being grown could reduce their numbers. **2.** Deposited atoms have to be incorporated into the correct positions in the growing semiconductor lattice. However, they may not take the lowest energy positions on the surface. In the case the atoms are deposited at higher free energy sites, the thermal energy may be insufficient to move them to a minimum free energy positions. **3.** The deposition rates and potential for the atomic constituents are required to be controlled so that the correct atoms are deposited in the correct order. For multinary system where this parameter is widely different, it becomes a subtle situation for the bath. The best approach to deal above issues of deposition has been attempted through ECALE as mentioned in the section 3.6. From the above discussion, it is therefore clear that, stringent control of ED parameters as well as post annealing could be a useful approach to produce *p*-type semiconductor thin film PV absorber layers.

4.1. Common procedures in electrodeposition of thin film solar cells

The electrodeposition followed by annealing (EDA) is a common procedure to for preparing good quality *p*-type compound semiconductors for solar cells. The primary purpose of the EDA is to form a reactive precursor film that can be converted to a compound semiconductor with the desired optoelectronic properties after a reactive annealing. For example, in the case where a compound chalcogenide film is required to be formed, the first step is to form an alloy layer or a stack of metal layers by ED, followed by annealing in a chalcogen atmosphere to

form the desired semiconductor compound. As another example, in the case where a stoichiometric semiconductor film is required, such as CdTe, the alloy itself is produced in ED step and air annealing may be used to control the conductivity type or to improve crystalline nature (such as by CdCl₂ anneal). The real challenge appears when ED is applied to deposit thin films at larger area such as a PV module. Maintaining desired stoichiometry and compositional uniformity in whole area requires additional skill and control. The nature of deposited layers depends on the film substrate, precursor species in solution, applied potentiodynamic scheme, mass-transfer condition and bath temperature. A brief description of each of these parameters is given below:

i. Nature of the substrate:

The substrate must be thoroughly cleaned, free of passivating oxides (if reactive to open air), and able to sustain the annealing conditions (should not soften or melt in post annealing). The substrate needs to be highly conducting to minimize the potential drop. Electrical contact to the substrate with electrode must not introduce any large resistance and also this contact must be sealed or protected from the solution environment.

ii. Use of precursors:

In many cases, such as in the chalcogenide compounds the films contain from two to five elements. There, the metal precursor ions may be available in one or more oxidation states, each of which has different solubility and reduction potentials. The metal ion can be introduced from their respective salt in case a common bath is used or supplied by anodic dissolution of a sacrificial anode in the case of sequential deposition. The metal ions can also be complexed with ligands to increase their solubility, prevent precipitation, and more importantly to narrow down the reduction potentials of various metal ions. Other components of the ED bath are supporting electrolytes which are inert during ED process but increase conductivity of the solution, acids, bases or pH buffers to control the solubility of the ionic species, and organic additives to control reaction rates or to improve the morphology of the deposits.

iii. Potentiodynamic condition:

Usually, different species of ion in solution has a different reduction potential. Theoretically, all the cations species can be reduced if the applied potential is made to a largest negative value to that of the ion species having largest negative reduction potential. However, such a deposit will be more likely in the form of binary and/or ternary compounds depending on the number of species in solution. Sometimes it leads to overgrowth or dendrite (fractal) formation of some elemental species (having lower reduction potential). Rather, by keeping the applied potential dynamic (potentiodynamic ED), this problem could be solved to some extent. It has been shown that use of a voltage sweep can assist the incorporation of electronegative elements and reduce any dendritic growth [83]. The work by Korger [84] suggest that, in a mixed ionic species system, the reduction potential of a more electronegative element in the compound may be shifted to positive, thermodynamically and a under-potential deposition condition may be achieved. Another common problem encountered during electrodeposition of ternary or quaternary chalcogen compounds is the presence of excess of the most noble metal (such as

Cu) in the film. This problem can be tackled either by reducing the concentration of the noble metal component to reduce its flux to the cathode surface, or by using an organic ligand to make complex of the metal ion in order to shift its reduction potential to more negative values.

iv. Mass transfer condition:

As different ion species are to be reduced at the electrode has different sizes, their transport in the solution, from diffusion to double layer region and from the double layer to be adsorbed on cathode after electron transfer is mass transfer limited process (kinetics depend on their mass directly). Therefore, their horizontal, vertical or convective (agitation in the bath or in Rotating Disk Electrode) motion will have direct impact on the final deposit.

v. Bath temperature:

An elevated bath temperature plays a key role to enhance surface diffusion of adatoms on the cathode surface in a cathodic ED. Due to enhanced adatom mobility on the surface, the crystalline quality of the film can be improved. However, the temperature must be optimized first as it may adversely affect other components, such as the metal-complex stability, adhesion of the film etc.

4.2. Review of electrodeposited-annealed (EDA) thin film PV absorbers

In the EDA scheme as defined in the previous section for the electrodeposition of p-type photovoltaic absorber thin films, four possible scheme of depositions are found in most of the literatures: (i) sequential deposition of metal layers (a stack), (ii) co-deposition of an alloy (to be post treated to form desired compound), (iii) stacks of binary and/or ternary compounds, and (iv) co-deposition of the compound as a whole as shown in Fig. 3.

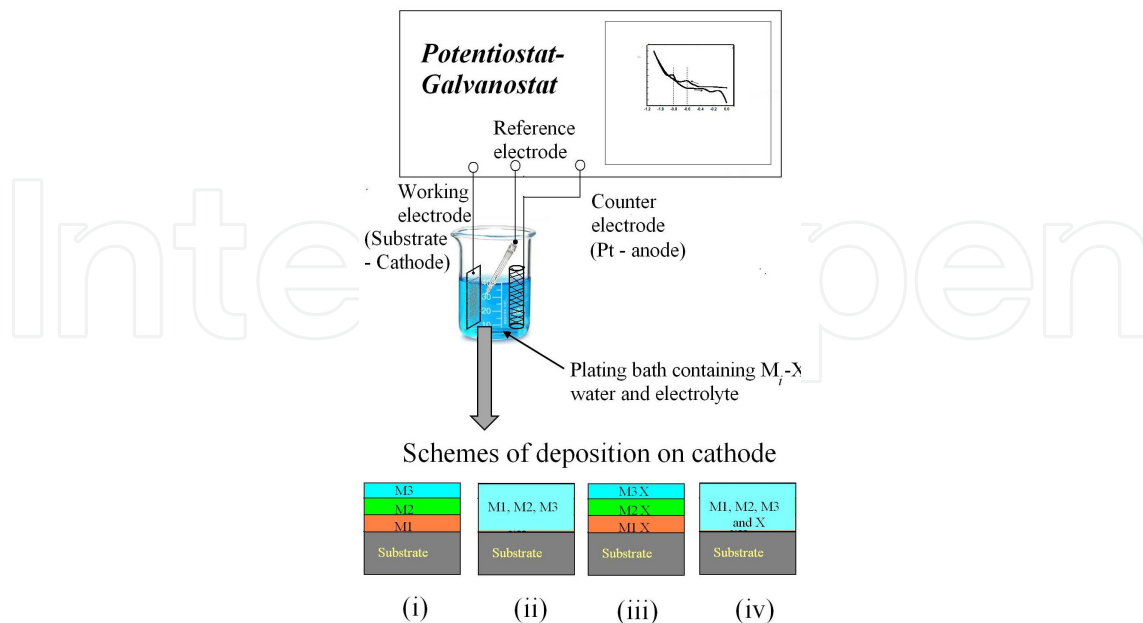


Figure 3. Schemes of cathodic electrodeposition of precursor film to be post annealed (EDA) for p-type photovoltaic absorber layers in literatures. Here, M_i represent constituent metal and X represents oxidized anion.

In the case (i) and (ii) above, the compound formation is done in post annealing step, when the anionic part (such as chalcogen for sulfides, selenides or telurides) reacts with the metal precursors at a higher temperature, and the semiconductor layer grows usually with larger grains [85]. The limitations of this method are poor adhesion, inclusion of cracks, blisters, and pinholes resulting from the substantial volume increase during the solid state reaction. Deposition of CIGS [86, 87] and CZTS [88-92] has been attempted with these two schemes.

The deposition of binary compounds in two/more layers in scheme (iii) is a mass transport limited process which may become complicated by the formation of several phases with different stoichiometries within a narrow range of experimental conditions. The binary stacks react together during annealing step, make phase transformation to produce large grains of the ternary/quaternary semiconductor compounds. One advantage of this method is that there are no large changes in volume during the formation of the ternary semiconductor. The layer of CuInSe₂ has been found to form with good optoelectronic properties in the case of EDA involving a Cu-Se and In-Se compound layers [83, 93].

Scheme (iv) of ED is performed in a single bath containing all cationic and anionic precursors and it has been attempted for all major classes of low cost PV absorbers including. CdTe [94,95], CIS [96,97], and CIGS [98]. This scheme of ED is much slower due to the lower concentrations of constituent used in solution. The process is difficult to control in the case of ternary or quaternary chalcogenides, however the subsequent annealing step in the presence of excess chalcogen may be used to further react secondary phases. Sometime, majority of secondary phases appear at the surface which are required to be removed by further surface treatment, such as through selective chemical etching.

A brief account of ED and EDA for majority of *p*-type photovoltaic absorbers, material-wise is given in following sub-sections.

4.2.1. Electrodeposition of CdTe

Electrodeposition of CdTe was attempted long back by Panicker *et al.* [74] where an aqueous solution containing excess of Cd²⁺ ions and TeO₂ was dissolved in acidic solution as HTeO₂⁺. Ni and Sb:SnO₂ transparent conducting glass were used as depositing electrode. The material was found to be n-type if pure solutions were used, whereas the presence of low concentration of copper impurities would produce p-type CdTe.

Thermodynamic aspects of cathodic electrodeposition have been discussed by Kroger [84], where the deposition potential of elemental Te and Cd can be obtained from the equilibrium potentials according to following reactions with accompanied Nernst equations:

Reaction	Corresponding deposition potential (vs. RHE)
$\text{HTeO}_2^+ + 3\text{H}^+ + 4e^- = \text{Te} + \text{H}_2\text{O}$	$E = 0.559 + 0.0148 \log[\text{HTeO}_2^+] - 0.0443 \text{ pH}$
$\text{Cd}_2^+ + 2e^- = \text{Cd}$	$E = -0.4025 + 0.0295 \log[\text{Cd}^{2+}]$

Reduction of Cd^{2+} needs a cathodic potential, again Te can be reduced at more cathodic potentials to form H_2Te as per following reaction:

Reaction	Corresponding deposition potential (vs. RHE)
$\text{Te} + 2\text{H}^+ + 2e^- = \text{H}_2\text{Te}$	$E = -0.740 - 0.0295 \log[\text{H}_2\text{Te}] - 0.059 \text{ pH}$

Finally, CdTe is deposited at a less cathodic potential according to:

Reaction	Corresponding deposition potential (vs. RHE)
$\text{Te} + \text{Cd}^{2+} + 2e^- = \text{CdTe}$	$E = 0.740 - 0.0295 \log[\text{Cd}^{2+}]$

At more cathodic potentials, CdTe can be reduced back to Cd and H_2Te according to:

Reaction	Corresponding deposition potential (vs. RHE)
$\text{CdTe} + 2\text{H}^+ + 2e^- = \text{Cd} + \text{H}_2\text{Te}$	$E = -1.217 - 0.0295 \log[\text{H}_2\text{Te}] - 0.059 \text{ pH}$

Therefore, the choice of potential is stringent by the regions in which CdTe is stable to both anodic and cathodic decomposition. In other word the CdTe deposition window is limited by the anodic limit of CdTe stability and by the cathodic deposition potential of bulk Cd.

Later, Basol *et al.* [99] had reported a CdS|CdTe heterojunction solar cell with 9.35% efficiency. They fabricated it by an EDA route, first electrodeposition of a CdS film onto indium tin oxide (ITO) coated glass followed by an electrodeposition of the CdTe layer. The layered structure was annealed at 400° C to finalize the heterojunction. CdTe deposition on TCO glasses was also studied by Rajeshwar *et al.* [100-103]. Later, its large-scale electrodeposition was first carried out by BP Solar [104] to achieve efficiencies above 10%. After 1984, a further research and development of CdTe electrodeposition was slowed down until recently, another breakthrough was found in electrodeposited CdTe in its post treatment by MgCl_2 by Major & coworkers [105] to achieve a new record of efficiency of 13%. Also, recently, Chauhan & co-worker have used ionic liquid based ED bath to deposit highly stoichiometric CdTe at lower process temperature [106].

4.2.2. Electrodeposition of CIS group of PV absorbers (CuInS_2 , CuIn(S, Se)_2 , Cu(InGa)Se_2)

The first ED attempt to produce a polycrystalline CuInSe_2 thin film of was reported by Bhattacharya [107] in which Cu, In, and Se were co-deposited from an acidic bath. Subsequently, EDA route with Cu-In alloys was attempted [108,109]. Bhattacharya *et al.* annealed electrodeposited In–Se/Cu – Se stacks [83]. The EDA routes which currently produce the most

efficient CuIn(S,Se)₂ solar cells involve co-deposition of all of the constituent elements in complex medium [110] followed by annealing in a sulfur containing atmosphere, and also the ED of a Cu–In alloy with a small amount of Se incorporation from ion species, followed by annealing in sulfur. Both routes have produced CIS solar cells with about 11% efficiency. As band gap optimization plays a crucial role to improve efficiency, in the case of CIS system incorporating Ga has been found most successful in physical vapor deposited layer [111]. Calixto *et al.* first reported Ga incorporation in ED films [112] by co-deposition route.

Further reports on the electrodeposition of CIGS were limited due to the difficulties in controlling the deposition kinetics of the four species of wide-ranging potentials. The standard reduction potential values of Se⁴⁺/Se, Cu²⁺/Cu, In³⁺/In and Ga³⁺/Ga are +0.740, +0.34, -0.34 and -0.53 V vs. Saturated Hydrogen Electrode (SHE), respectively. The deposition potential of elemental Cu, In, Ga and Se, in case of electrodeposition of Cu(In,Ga)Se₂ can be obtained from the equilibrium potentials according to following reactions with accompanied Nernst equations:

Reaction	Corresponding deposition potential (vs. RHE)
$\text{Cu}^{2+} + 2e^- \leftrightarrow \text{Cu}$	$V_{\text{Cu}^{2+}/\text{Cu}} = 0.34 + 0.0295 \log (a_{\text{Cu}^{2+}} / a_{\text{Cu}})$
$\text{In}^{3+} + 3e^- \leftrightarrow \text{In}$	$V_{\text{In}^{3+}/\text{In}} = -0.34 + 0.0197 \log (a_{\text{In}^{3+}} / a_{\text{In}})$
$\text{Ga}^{3+} + 3e^- \leftrightarrow \text{Ga}$	$V_{\text{Ga}^{3+}/\text{Ga}} = -0.53 + 0.0197 \log (a_{\text{Ga}^{3+}} / a_{\text{Ga}})$
$\text{HSeO}_2^+ + 4\text{H}^+ + 4e^- + \text{OH}^-$ \leftrightarrow $\text{HSeO}_3 + 4\text{H}^+ + 4e^-$ \leftrightarrow $\text{Se} + 3\text{H}_2\text{O}$	$V_{\text{H}_2\text{SeO}_3/\text{Se}} = V_{\text{H}_2\text{SeO}_3/\text{Se}}^0 +$ $+\left(\frac{RT}{4F}\right) \log (a_{\text{HSeO}_2^+} / a_{\text{Se}}) +$ $+\left(\frac{3RT}{4F}\right) \log (C_{\text{H}^+}) =$ $= 0.74 + 0.0148 \log (a_{\text{HSeO}_2^+} / a_{\text{Se}}) - 0.0433 \text{ pH}$

In above expressions, 'a' refers to activity, for ions it is proportional to concentration of the respective ion and for pure elements it is considered to be unity.

This leads to a preferential deposition of single element causing overgrowing local non-stoichiometry. Due to the more negative reduction potential of Ga, its incorporation into the lattice becomes difficult. However, the best ED CIGS was reported by Kampmann *et al.* with a device efficiency of over 10% where they used a stacked layered scheme of ED [113]. The CIGS layer can be co-electrodeposited or it can be formed by a two stage approach. In co-deposition, the concentration and pH of the electrolyte needs to be adjusted or complex may be considered such that the electrode potentials of all the individual elements become closer to each other. The two stage strategy can be employed via stacked layer scheme with binary or ternary films, followed by an annealing in Se or S [114,115]. Co-deposition route is often preferred to reduce the harmful emissions, however, the prevailing factors in the co-deposition are largely: (i) the electrode potentials of individual ions in the electrolyte, (ii) cathodic polarization caused by the difference in deposition. potentials, (iii) relative ion concentrations

in the electrolyte, (iv) the dissolution chances, and (v) the hydrogen overpotential on the deposited cathode surface. In most cases, the as-deposited films are found to be poorly crystalline and may consist of Cu–Se second phases, which may be reduced by a post-annealing treatment and brings about stoichiometry. Usually, the Cu/(In + Ga) and Ga/(In + Ga) ratios are critical in determining the cell performance [96]. Readers may refer to some of the well written reviews on electrodeposited CIS/CIGS solar cells for further details of synthesis and characterizations [117-121].

4.2.3. Electrodeposition of CZTS

An earth-abundant and environmentally benign $\text{Cu}_2\text{ZnSnS}_4$ (CZTS) are one of the ideal candidates for the production of thin film solar cells at large scale due to the large natural abundance of all the elements, a direct band gap in the range of 1.45–1.6 eV [122,123], a high optical absorption coefficient of around 10^5 cm^{-1} and *p*-type semiconductor that matches well with the solar spectrum, and it has achieved a benchmark power conversion efficiency of more than 10% [124,125]. In EDA scheme, first the cathodic electrodeposition of constituent Cu, Zn and Sn can be expressed in following sets of reduction reactions and accompanied Nernst equations:

Reaction	Corresponding deposition potential (vs. RHE)
$\text{Cu}^{2+} + 2e \leftrightarrow \text{Cu}$	$E_{\text{Cu}^{2+} \rightarrow \text{Cu}} = 0.34 + 0.0295 \log[\text{Cu}^{2+}]$
$\text{Zn}^{2+} + 2e \leftrightarrow \text{Zn}$	$E_{\text{Zn}^{2+} \rightarrow \text{Zn}} = -0.76 + 0.0295 \log[\text{Zn}^{2+}]$
$\text{Sn}^{2+} + 2e \leftrightarrow \text{Sn}$	$E_{\text{Sn}^{2+} \rightarrow \text{Sn}} = -0.14 + 0.0295 \log[\text{Sn}^{2+}]$

Ennaoui *et al.* first reported a co-electrodeposition scheme for $\text{Cu}_2\text{ZnSnSe}_4$ alloy that was post-annealed using under H_2S environment at 550 °C for 2 h and the resulting solar cell showed an efficiency of 3.4% [126]. Addition of selenium to the system results in a band gap-lowering that helps to get a higher current density. Later, Scragg *et al.* attempted an EDA route with an electrodeposited metallic stack of Cu/Sn/Cu/Zn and its subsequent annealing in a sulfur-containing atmosphere mixed with 10% H_2/N_2 and heated to 575 °C for 2h to achieve a solar cell efficiency of 3.2% [127]. Redinger *et al.* in a novel approach annealed Cu and Zn precursor in a gas containing SnS and SnSe for 2 h at 540 °C to achieve efficiency 5.4% [128]. They pointed out that during annealing of a Cu/Zn precursor in the presence of SnS and SnSe vapor, the partial pressure of SnS and SnSe shifts the reaction equilibrium towards the formation of a single-phase $\text{Cu}_2\text{ZnSn}(\text{S,Se})_4$ without Sn loss. However, a key drawback to some of the previous technique was longer duration of annealing, which is not desirable for commercial production of such CZTS absorbers. To address this issue, Zhang *et al.* [129] considered co-deposition of Cu-Zn-Sn in single bath followed by a rapid thermal annealing in Se atmosphere to obtain CZTSe solar cell with 4.5% power conversion efficiency. In a more deliberate study for CZTS system, Ahmed *et al.* [130] reported a shorter duration EDA route, where the metals stack of copper, zinc, and tin was sequentially electroplated on 600 nm sputtered molybdenum

layer on soda lime glass substrate and annealed at low temperature (210–350 °C) in order to convert the elemental metals to metal alloys of CuSn and CuZn. After the formation of the homogeneous alloy of CuZn and CuSn layer, the film was given heat treatment at 585 °C for 12 min in a sealed quartz tube with 2–5 mg elementary sulfur under nitrogen atmosphere. In this study, they reported a champion $\text{Cu}_2\text{ZnSnS}_4$ solar cell with power conversion efficiency of 7.3%. The record efficiency is still below the bench mark at 11% obtained for CZTS solar cell by vacuum process [131]. One of the reasons could be the morphology and greater secondary phase fraction in EDA processed film. However, this efficiency can be improved further by considering other aspects of the solar cell device, such as reducing series resistance at the back contact, increasing shunt resistance by lowering deep level impurities, improving current density by reducing reflection and band-gap engineering and improving the open circuit voltage by thickness optimization and doping control.

4.2.4. Electrodeposition of other low cost PV

Other than the conventional non-silicon based earth abundant photovoltaic absorber, Zn_3P_2 is another promising compound semiconductor having a direct band gap of 1.5 eV [132]. Wyeth and Catalano [133] investigated the Schottky junction properties of Zn_3P_2 with various metals, and solar cells were constructed using metal/ Zn_3P_2 Schottky contact by some researchers. The Mg/ Zn_3P_2 solar cell shows the power conversion efficiency of 6% when the film was fabricated by gas phase growth, e.g. evaporation [134,135], MOCVD [136,137] and RF-sputtering [138]. Soliman *et al.* first reported an electrodeposited of Zn_3P_2 from aqueous solution containing zinc and phosphorus species [139] at normal temperatures and pressures. Later, Nose *et al.* reported electrodeposited Zn_3P_2 from aqueous solution where they constructed the Pourbaix (potential-pH) diagram of the Zn-P- H_2O system at 363 K and clarified the wide stable region of Zn_3P_2 at lower potentials [140]. They showed that, in order to obtain Zn_3P_2 by electrodeposition from aqueous solutions, it is necessary that the reduction of Zn^{2+} is suppressed and that of phosphate ions is enhanced.

5. Electrodeposition applied to dye sensitized solar cells

Dye Sensitized Solar Cell (DSSC)s are the classes of low cost photovoltaic device where a dye molecule (inorganic or organic) contributes to photoexcitation and transfer the photo-excited electron to the conduction band (CB) of a semiconductor having CB edge energetically favorable to accept the photo-excited electrons. Organic dye and pigment molecules are important class of materials for enhanced optical absorption in DSSCs due to their large oscillator strengths in aromatic systems. Therefore a lower film thickness can be adopted without compromising much on the efficiency. Two important approaches in this direction have been considered in DSSCs: (i) the use of multiple ultrathin films of high structural control using doping of layers to decrease the series resistance and (ii) the use of bulk heterojunctions consisting of a conductive pathway of a crystalline organic acceptor with large interfacial contact area to a matrix of a donor conductive polymer, prepared from a mixed solution of both constituents. An alternative way to make use of the strong absorption of organic dye

molecules is realized in DSSCs [141,142] consisting of a porous wide-band gap semiconductor as electron-conducting phase, the organic dye as absorber, and a hole-conducting medium (typically iodine). The electron transport to the electrode in DSSCs is conventionally done by a TiO_2 layer. However, more economic solution at large scale could be to use ZnO as an alternative to TiO_2 . The reason behind to consider ZnO is its versatility to form various forms of nanostructure and can be easily prepared by electrodeposition routes. The DSSCs can be realized based on porous ZnO as a wide-band gap semiconductor. As a post annealing step is not required, in general to obtain well-crystallized ZnO various types of substrates can be used. Additionally, ZnO as a thin film after Al-doping, Al:ZnO (AZO) serves as a transparent conductive oxide to replace more costly indium tin oxide (ITO) which is mainly due to the scarcity of In [89]. Other than the cost, another limitation of ITOs is inherent brittleness, that bars them to be grown on flexible substrates. In this aspect, the viability of ED of ZnO on flexible substrates can be appreciated. The combination of a compact AZO back electrode with electrodeposited porous ZnO layers for dye sensitization represents a very promising DSSC component with the prospect of low interface defects and production costs [143]. Different precursor routes have been attempted [144] to cathodically electrodeposit ZnO from aqueous electrolytes containing O_2 , or NO_3^- , or H_2O_2 as the source of oxygen. By reduction at the cathode, the $[\text{-OH}]$ concentration rises in the solution. The reactions best describing this cathodic process can therefore be written as:



Such an increase in pH leads to a situation when the solubility product of $\text{Zn}(\text{OH})_2$ or ZnO is exceeded and a condition of supersaturation is achieved [69]. In the presence of appropriate crystallization seeds ZnO crystals nucleate and grow under controlled conditions. Readers may refer to the review by Yoshida and Schlettwein for further details of various possible hybrid inorganic-ZnO/ organic-dye structures applied to DSSCs [145], critical consideration of ZnO ED schemes by Yoshida et al. [146] and the detailed study of the role of structure directing agent by the same group with other workers [147]

6. Non-conventional electrodeposition: Electrodeposition from non-aqueous and ionic liquid bath

In the electrodeposition from aqueous solution, precursor films suffer from a number of problems. For example, in the case of CuInS_2 or $\text{Cu}(\text{In,Ga})\text{S}_2$, the incorporation of In or Ga is

not an easy task. Due to their limited solubility and large negative reduction potentials (very close to the hydrogen evolution reaction (HER) of water), it becomes necessary to use strong complexing agent to shift the reduction potential at more positive values. This may require toxic ligands, such as cyanide and to work under highly alkaline conditions to avoid HER which causes extremely poor morphology of the deposits. More unfortunately, In and Ga are often deposited together with their oxide or hydroxide forms under these conditions. A possible solution to these problems could be to replace the aqueous deposition medium by room temperature ionic liquids (RTIL). RTILs are defined as liquids consisting of molecular cations and anions that have a melting point below 100°C with ultra low vapor pressure. Due to the size of the molecular ions and the fact that the charge is delocalized through the molecule, RTILs have wide electrochemical windows. The ultra low vapor pressure and high degradation temperature allow them to be used at temperatures up to 250°C. The electrochemical window of most common pyrrolidinium-based RTILs are between 5 and 6 V [148]. Shivagan *et al.* [159] have shown that In and Ga can be reversibly electrodeposited from a eutectic based RTIL composed of a 1:2 choline chloride: urea mixture. El Abedin *et al.* studied the electrochemistry of Cu, In, and Se, individually in the 1-butyl-1-methylpyrrolidinium-bis(trifluoromethylsulfonyl)amide RTIL [150]. This group also showed that Ga can be deposited electrochemically on Au(111) electrodes [151] with this RTIL used. The high temperature ED using RTIL is interesting because a better crystallinity of the deposited films can be expected even without post heat treatment. Yang *et al.* [152] showed that for the electrodeposition of InSb from 1-ethyl-3-methylimidazolium chloride/tetrafluoroborate, at temperatures up to 120°C and the crystallinity of InSb film increased with the deposition temperature. The as-deposited InSb films were p-type and highly photoactive. First CdTe deposition onto glassy carbon, titanium, and tungsten substrates from 1-ethyl-3-methylimidazolium chloride/tetrafluoroborate in RTIL was carried out by Hsiu *et al.* at 140°C [153]. Chauhan *et al.* [106] demonstrated that highly stoichiometric p-type CdTe absorber can be grown using BMIM Cl⁻ RTIL bath. The electrodeposited p-CZTS absorber layer from RTIL was first attempted by Chan *et al.* using a eutectic mixture of choline chloride and ethylene glycol at a molar ratio of 1:2 [154] where Cu, Sn and Zn could be deposited at potentials -0.55V, -0.67V and -1.1V (vs. Ag/AgCl) in a cathodic scan. The resulting CZTS film after annealing was highly crystalline and free from the incorporation of oxide impurities that usually appears in the case of aqueous medium.

7. Conclusions

Electrodeposition, a low cost non-vacuum technique for fabrication of thin films deserves its place in the development of next generation solar cells and modules. Owing to its simplicity and scalability, various compound semiconductor photovoltaic absorbers, such as $\text{Cu}_2\text{ZnSnS}_4$, Cu_2S , SnS , Cu_2SnS_3 *etc.* have already been fabricated at lab and pilot scales. Although, these photovoltaic absorbers may suffer poor phase purity and crystalline nature, controlling the deposition parameters and surface functionalization of the deposited layer can help achieve ultra low cost and environment friendly thin film solar cells and modules.

Author details

Abhijit Ray*

Address all correspondence to: abhijit.ray1974@gmail.com

School of Solar Energy, Pandit Deendayal Petroleum University, Raisan, Gandhinagar, Gujarat, India

References

- [1] Fthenakis V. (2009). *Ren. Sust. Energy Rev.* 13(9), 2746–2750.
- [2] Alonso, E., et al. (2007). *Env. Sci. & Technol.* 41(19), 6649–6656.
- [3] Ginley, D., et al. (2008). *MRS Bull.* 33, 355.
- [4] Habas, S.E., et al. (2010). *Chem. Rev.* 110, 6571–6594.
- [5] Würfel, P. and Würfel, U. (2009). *Physics of solar cells: from basic principles to advanced concepts.* John Wiley & Sons.
- [6] T. Unold and H.W. Schock. (2011). *Annu. Rev. Mater. Res.* 41, 297.
- [7] Chopra, K. L. and Das, S.R. (1983). *Why Thin Film Solar Cells?*. Springer, USA.
- [8] López, N., et al. (2011). *Phys. Rev. Lett.* 106.2, 028701.
- [9] Shafarman, W. N., Klenk, R. and McCandless, B.E. (1996). *J. Appl. Phys.* 79.9, 7324-7328.
- [10] Romeo, N., et al. (1999). *Solar Energy Mater. Sol. Cells* 58.2, 209-218.
- [11] Guillemoles, J-F., et al. (2000). *J. Phys. Chem. B*, 104.20 (2000): 4849-4862.
- [12] Fujii, M., et al. (1988). *Solar Energy Mater.*, 18, 23.
- [13] Romeo, N., et al. (1978) *Appl. Phys. Lett.*, 32, 807.
- [14] Jones, A. C. (1997). *Chem. Soc. ReV.*, 26, 101.
- [15] O'Brien et al. (1996). *J. Cryst. Growth*, 167, 133.
- [16] Fainer et al. (1996). *Thin Solid Films*, 280, 16.
- [17] Cheon et al. (1997). *J. Am. Chem. Soc.*, 119, 3838.
- [18] Fujita, S., et al. (1996). *Cryst. Growth*, 164, 196.
- [19] Fraser, D. B. and Melchior, H. J. (1972). *Appl. Phys.*, 43, 3120.

- [20] Liu et al. (1994). *J. Appl. Phys.*, 75, 3098.
- [21] Meng et al. (1995). *Vacuum* 1995, 46, 1001
- [22] Asom, M. T., et al. (1991). *J. Crystal Growth* 112.2, 597-599.
- [23] Fraas, L. M., et al. (1986). *J. Electron. Mater.* 15.3, 175-180.
- [24] Sivakov, V., et al. (2009). *Nano Lett.* 9.4, 1549-1554.
- [25] Gur, I., et al. (2005). *Science* 310.5747, 462-465.
- [26] Kyoohee, W., et al. (2012). *Energy & Env. Sci.* 5.1, 5340-5345.
- [27] Maeda K, et al. (2011) *Solar Energy Mater. Sol. Cells* 95: 2855–2860.
- [28] Akhavan, V.A., et al. (2012). *J. Solid State Chem.* 189, 2–12.
- [29] Woo K, Kim Y, Moon J. (2012). *Energy Environ. Sci.* 5: 5340-5345
- [30] Rajeshmon, V.G., et al. (2011). *Solar Energy* 85, 249–255.
- [31] Das, S., et al. (2012). *ECS Trans.* 45 (7), 153-161.
- [32] Patel, M., et al. (2012). *J. Phys. D: Appl. Phys.* 45, 445103.
- [33] Mali. S.S., et al. (2012). *Electrochim. Acta.* 66, 216– 221.
- [34] Wangperawong, A., et al. (2011). *Thin Solid Films* 519, 2488–2492.
- [35] Scragg, J.J., et al. (2010). *J. Electroan. Chem.* 646, 52–59.
- [36] Ennaoui, A., et al. (2009). *Thin Solid Films* 517: 2511–2514.
- [37] Lincot, D. (2005). *Thin Solid Films* 487.1, 40-48.
- [38] Fulop, G. F. and Taylor, R.M. (1985). *Annual Rev. Mater. Sci.* 15.1, 197-210.
- [39] Gary, H., ed. (2008). *Electrochemistry of Nanomaterials*. John Wiley & Sons.
- [40] Ruythooren, W., et al. (2000). *J. Micromech. Microengg.* 10.2, 101.
- [41] Dharmadasa, I. M., and Haigh, J. (2006). *Journal of The Electrochemical Society* 153.1, G47-G52.
- [42] Scragg, J.J., et al. (2008). *Electrochem. Commun.* 10.4, 639-642
- [43] Paunovic, M. and Schlesinger, M. (2006). *FUNDAMENTALS OF ELECTROCHEMICAL DEPOSITION*, Wiley Interscience, 2nd Ed., New Jersey.
- [44] J. Choi, R. B. et al. (2004). *Electrochim. Acta*, 49, 2645.
- [45] Y. T. Sul, et al. (2001). *Medical Engg. Phys.*, 23, 329.
- [46] Feng, X., et al. (2008). *Nano Letters*, 8.11, 3781-3786.
- [47] Baxter, J. B., et al. (2006). *Nanotechnology*, 17.11, S304.

- [48] Mor, G. K., et al. (2005). *Adv. Func. Mater.* 15.8, 1291-1296.
- [49] Yu, X., et al. (2008). *Sensors and Actuators B: Chemical*, 130.1, 25-31.
- [50] Chu, S-Z., et al. (2005). *Adv. Func. Mater.* 15.8, 1343-1349.
- [51] Mor, G. K., et al. (2006). *Nano Letters* 6.2, 215-218.
- [52] Paulose, M., et al. (2006). *J. Phys. D: Appl. Phys.* 39.12, 2498.
- [53] Leenheer, A. J., et al. (2007). *J. Mater. Res.* 22.03, 681-687.
- [54] Macak, J. M., et al. (2006). *Chem. Phys. Lett.* 428.4, 421-425.
- [55] Premchand, Y. D., et al. (2006). *Electrochem. Commun.* 8.12, 1840-1844.
- [56] Yu, X., et al. (2006) *Nanotechnology* 17.3, 808.
- [57] Huang, H., et al. (2013). *Energy Environ. Sci.* 6.10, 2965-2971.
- [58] Wang, C. E., et al. (2014). *J. Mater. Sci. Nanotech.* 1.1, 1.
- [59] Owen, J. I., et al. (2011). *Phys. status solidi (a)* 208.1, 109-113.
- [60] Dennison, S., (1993). *Electrochim. Acta* 38, 2395.
- [61] H. Gobrecht, H.D., et al. (1973). *Phys. Chem.* 67, 930.
- [62] Pourbaix, M., (1974). *Atlas of electrochemical equilibria in aqueous solutions*. National association of corrosion engineers (2nd English Edn.) USA.
- [63] Savadogo, O., (1998). *Solar Energy Mater Sol. Cells* 52, 361-388.
- [64] Dremlyuzhenko, S.G., et al. (2008). *Inorg Mater* 44, 21-29.
- [65] Bouroushian, M., (2010). *Electrochemistry of Metal Chalcogenides*, Springer-Verlag Berlin Heidelberg.
- [66] Tsao, J. Y., (1993). *Materials Fundamentals of Molecular Beam Epitaxy*, Academic Press, London.
- [67] Stringfellow, G. B., (1989). *Organometallic Vapor-Phase Epitaxy: Theory and Practice* Academic Press, Inc., London.
- [68] Sze, S. M. (1985). *Semiconductor Devices Physics and Technology*.
- [69] Gregory, B.W. and Stickney, J.L. (1991). *J. Electroanal. Chem.* 300, 543.
- [70] Innocenti, M., et al. (2001). *J. Electrochem. Soc.* 148.5, C357-C362.
- [71] Pezzatini, G., et al. (1999). *J. Electroanal. Chem.*, 475, 164.
- [72] Gregory, B. W., et al. (1990). *J. Electroanal. Chem.*, 293, 85.
- [73] Gregory, B. W. and Stickney, J. L. (1991). *J. Electroanal. Chem.*, 300, 543.

- [74] Demir, U. and Shannon, C. (1994). *Langmuir*, 10, 2794.
- [75] Streltsov, E. S., et al. (1994). *Dokl. Akad. Nauk Bel.*, 38, 64.
- [76] Foresti, M. L. et al. (1998). *J. Phys. Chem. B* 102, 38, 7413.
- [77] Wade, T. L., et al. (1999). *Electrochem. Solid-State Lett.*, 2, 616.
- [78] Innocenti, M., et al. (2001). *Electroanal. Chem.*, 514, 75.
- [79] Colletti, L. P. and Stickney, J. L. (1995). Abstracts of the 210th ACS National Meeting, Chicago, IL, August 20-24, 1995, (Pt. 1), INOR-297.
- [80] Technology Roadmap, Solar photovoltaic energy, IEA Publication, 2014.
- [81] Holden, N. E., "Table of the Isotopes", in Lide, D. R., Ed., *CRC Handbook of Chemistry and Physics*, 86th Ed., CRC Press, Boca Raton FL, 2005.
- [82] Alharbi, F. et al. (2011). *Renewable Energy* 36, 2753e2758.
- [83] Bhattacharya, R.N., et al. (1996) *J. Electrochem. Soc.*, 143, 854.
- [84] Kroger, F.A. (1978). *J. Electrochem. Soc.*, 125, 2028.
- [85] Voss, T., et al. (2007). 22nd European Photovoltaic Solar Energy Conference, 3 – 7 September 2007, Milan.
- [86] Zank, J., et al. (1996). *Thin Solid Films*, 286, 259.
- [87] Kampmann, A., et al. (2003). *Proceeding of the MRS Spring Meeting*, San Francisco.
- [88] Scragg, J.J., et al. (2010). *J. Electroanal. Chem.*, 646, 52.
- [89] Scragg, J.J., et al. (2008). *Electrochem. Commun.*, 10, 639.
- [90] Scragg, J.J., et al. (2009). *Thin Solid Films*, 517, 2481.
- [91] Scragg, J.J., et al. (2008). *Phys. Stat. Sol. (b)*, 245, 1772.
- [92] Araki, H., et al. (2009). *Solar Energy Mater. Solar Cells*, 93, 996.
- [93] Guillen, C. and Herrero, J. (1996). *J. Electrochem. Soc.*, 143, 493 – 8.
- [94] Panicker, M.P.R., et al. (1978). *J. Electrochem. Soc.*, 125, 566.
- [95] Basol, B.M. and Tseng, E.S.F. (1983). *J. Electrochem. Soc.*, 130, C243.
- [96] Dale, P.J., et al. (2008). *J. Phys. D*, 41, 085105.
- [97] Lincot, D. et al (2004). *Solar Energy*, 77, 725.
- [98] Calixto, M.E., et al. (2005). *Conference Record of the 31st IEEE Photovoltaic Specialists Conference*, p. 378.
- [99] Basol, B.M., et al. (1984). *J. Appl. Phys.*, 58, 3809.

- [100] Rajeshwar, K., and Bhattacharya, R.N. (1984). *J. Electrochem. Soc.*, 131, C314.
- [101] Rajeshwar, K., et al. (1984). *J. Electrochem. Soc.*, 131, C313.
- [102] Bhattacharya, R.N. and Rajeshwar, K. (1985). *J. Appl. Phys.*, 58, 3590.
- [103] Bhattacharya, R.N., et al. (1985). *J. Electrochem. Soc.*, 132, 732.
- [104] Turner, A.K. et al, (1994). *Solar Energy Mater. Sol. Cells*, 35, 263.
- [105] Major, J. D., et al. (2014). *Nature* 511, 334-337.
- [106] Chauhan, K.R. et al. (2014). *J. Electroanal. Chem.* 713, 70–76.
- [107] Bhattacharya, R.N. (1983) *J. Electrochem. Soc.*, 130, 2040.
- [108] Hodes, G., et al. (1985). *Thin Solid Films*, 128, 93.
- [109] Kapur, V.K., et al. (1987) *Solar Cells*, 21, 65 – 72.
- [110] Kessler et al. (2005) 20th European Photovoltaic Solar Energy Conference, 6 – 10 June 2005, Barcelona.
- [111] Bar, M., et al. (2009) *Appl. Phys. Lett.*, 95, 3.
- [112] Calixto, M.E., et al. (1999) *Solar Energy Mater. Sol. Cells*, 59, 75.
- [113] Kampmann, A., et al. (2003) *Proceeding of the MRS Spring Meeting*, San Francisco.
- [114] Zank, J., et al. (1996). *Thin Solid Films* 286, 259–263.
- [115] Friedfeld, R., et al. (1999). *Solar Energy Mater. Sol. Cells* 58, 375–385.
- [116] Bhattacharya, et al. (1998) *Solar Energy Mater. Sol. Cells* 55, 83–94.
- [117] Lincot, D., et al. (2004). *Sol. Energy* 77, 725–737.
- [118] Kaelin, M., et al. (2004) *Sol. Energy* 77, 749–756.
- [119] Lincot, D., (2005). *Thin Solid Films* 487, 40–48.
- [120] Hibberd, C.J., et al. (2010). *Prog. Photovolt. Res. Appl.* 18, 434–452.
- [121] Saji, V.S., et al. (2011). *Solar Energy* 85, 2666–2678.
- [122] Jimbo, K. et al. (2007). *Thin Solid Films*, 515, 5997.
- [123] Ito, K. and Nakazawa, T. (1988). *Jpn. J. Appl. Phys.* 27, 2094.
- [124] Mitzi, D.B. et al. (2011). *Sol. Energy Mater. Sol. Cells*, 95, 1421.
- [125] Todorov, T.K. et al. (2010). *Adv. Mater.* 22, 1.
- [126] Ennaoui, A., et al. (2009). *Thin Solid Films*, 517, 2511–2514.
- [127] Scragg, J. J., et al. (2010). *J. Electroanal. Chem.*, 646, 52.

- [128] Redinger, A., et al. (2011). *J. Am. Chem. Soc.* 2011, 133, 332.
- [129] Zhang, Y.Z., et al. (2013) *Solar Energy*, 94, 1-7.
- [130] Ahmed, S., et al. (2012). *Adv. Energy Mater.*, 2, 253–259.
- [131] Torodov, T.K. et al. (2013). *Adv. Energy Mater.* 3, 34–38.
- [132] Fagen, E. A., (1979). *J. Appl. Phys.*, 50, 6505
- [133] Wyeth, N. C. and Catalano, A. (1980). *J. Appl. Phys.*, 51, 2286
- [134] Lousa, A. et al. (1985). *Sol. Energy Mater.*, 12, 51
- [135] Murali, K. R., (1987) *Mater. Sci. Eng.*, 92, 193.
- [136] Long, J. (1983). *J. Electrochem. Soc.*, 130, 725.
- [137] Hermann, A. M., et al. (2004). *Sol. Energy Mater. Sol. Cells*, 82, 241
- [138] Suda, T., et al. (1988). *J. Cryst. Growth*, 86, 423
- [139] Soliman, M., et al. (2005). *Renewable Energy*, 30, 1819
- [140] Nose, Y., et al., (2012). *Journal of The Electrochemical Society*, 159 (4) D181-D186
- [141] Hagfeldt, A. and Grätzel, M. (2000) *Molecular photovoltaics. Acc. Chem. Res.*, 33 (5), 269 – 277.
- [142] Grätzel, M. (2001). *Nature*, 414, 338 – 344.
- [143] Loewenstein, T., et al. (2008). *Phys. Stat. Sol. (a)*, 205, 2382 – 2387.
- [144] *Advances in Electrochemical Science and Engineering*, Edited by Richard C. Alkire, Dieter M. Kolb, Jacek Lipkowski, and Philip N. Ross, Wiley (2010).
- [145] Yoshida, T. and Schlettwein, D. (2004) *Electrochemical self - assembly of oxide/ dye composites*, in *Encyclopedia of Nanoscience and Nanotechnology*, vol. 2 (ed. A. Nalwa), American Scientific Publishers, Stevenson Ranch, pp. 819 – 836.
- [146] Yoshida, T., et al., (1999). *Chem. Mater.*, 11, 2657 – 2667.
- [147] Yoshida, T., et al., (2002). *Electrochemistry*, 70, 470 – 487
- [148] Abedin, S.Z.E. and Endres, F. (2006) *Chem.Phys.Chem.*, 7, 58.
- [149] Shivagan, D.D., et al. (2007). *Thin Solid Films*, 515, 5899.
- [150] Abedin, S.Z.E., et al. (2007) *Electrochim. Acta*, 52, 2746.
- [151] Gasparotto, L.H.S., et al. (2009) *Electrochim. Acta*, 55, 218.
- [152] Yang, M.H., et al. (2003) *J. Electrochem. Soc.*, 150, C544.
- [153] Hsiu, S.I. and Sun, I.W. (2004) *J. Appl. Electrochem.*, 34, 1057.

- [154] Chan, C.P., et al., (2010). *Solar Energy Mater. Sol. Cell* 94, 207
- [155] Anuar, K., et al. (2002). *Solar Energy Mater. Sol. Cell.* 73, 351.
- [156] Koike, J., et al. (2012). *Jap. J. Appl. Phys.* 51.10S, 10NC34.
- [157] Mathews, N. R., et al. (2013) *J. Mater. Sci.: Mater. Electron.* 24.10, 4060-4067.
- [158] Yong-Sheng, C., et al. (2012) *Chinese Phys. B* 21.5, 058801.
- [159] Cui, Y., et al. (2011) *Solar Energy Mater. Sol. Cells* 95.8, 2136-2140.
- [160] Pawar, B. S., et al. (2011). *ISRN Renewable Energy* 2011.
- [161] Jeon, J-O., et al. (2014). *ChemSusChem* 7.4, 1073-1077.
- [162] Guo, L., et al. (2014). *Prog. Photovoltaics: Res. Appli.* 22.1 (2014): 58-68.
- [163] Septina, W., et al. (2013). *Electrochimica Acta* 88, 436-442.
- [164] Li, J., et al. (2012) *Appl. Surf. Sci.* 258.17, 6261-6265.
- [165] Steichen, M. et al. (2013). *J. Phys. Chem. C*, 117 (9), 4383-4393.
- [166] Ghazali, A., et al. (1998). *Solar Energy Mater. Sol. Cells*, 55.3, 237-249.
- [167] Subramanian, B., et al. (2001). *Mater. Chem. Phys.*, 71.1, 40-46.
- [168] Zainal, Z., (1996). *Solar Energy Mater. Sol. Cells*, 40.4 (1996): 347-357.
- [169] Cheng, S., et al. (2006) *Thin Solid Films* 500.1, 96-100.
- [170] Cheng, Shuying, et al. (2007). *Mater. Lett.* 61.6, 1408-1412.
- [171] Cheng, Shuying, et al. (2006). *Opt. Mater.* 29.4, 439-444.
- [172] Mkawi, E. M., et al. (2014). *Solar Energy Mater. Sol. Cells* 130, 91-98.

